



Published in final edited form as:

Chem Res Toxicol. 2012 September 17; 25(9): 1975–1984. doi:10.1021/tx300283t.

The marine algal toxin azaspiracid is an open state blocker of hERG potassium channels

Michael J. Twiner^{†,*}, Gregory J. Doucette[‡], Andrew Rasky[†], Xi-Ping Huang[§], Bryan L. Roth[§], and Michael C. Sanguinetti[¶]

[†]Department of Natural Sciences, University of Michigan – Dearborn, Dearborn, MI USA

[‡]Marine Biotoxins Program, NOAA/National Ocean Service, Charleston, SC USA

[§]Department of Pharmacology and Division of Chemical Biology and Medicinal Chemistry, University of North Carolina at Chapel Hill Medical School, Chapel Hill, NC USA

[¶]Departments of Medicine and Physiology, and Nora Eccles Harrison Cardiovascular Research and Training Institute, University of Utah, Salt Lake City, Utah USA

Abstract

Azaspiracids (AZA) are polyether marine dinoflagellate toxins that accumulate in shellfish and represent an emerging human health risk. Although human exposure is primarily manifested by severe and protracted diarrhea, this toxin class has been shown to be highly cytotoxic, a teratogen to developing fish, and a possible carcinogen in mice. Until now, AZA's molecular target(s) has not yet been determined. Using three independent methods (voltage clamp, channel binding assay, and thallium flux assay), we have for the first time demonstrated that AZA1, AZA2, and AZA3 each bind to and block the hERG (human *ether-à-go-go* related gene) potassium channel heterologously expressed in HEK-293 mammalian cells. Inhibition of K⁺ current for each AZA analogue was concentration-dependent (IC₅₀ value range: 0.64 - 0.84 μM). The mechanism of hERG channel inhibition by AZA1 was investigated further in *Xenopus* oocytes where it was shown to be an open state-dependent blocker and, using mutant channels, to interact with F656 but not with Y652 within the S6 transmembrane domain that forms the channel's central pore. AZA1, AZA2, and AZA3 were each shown to inhibit [³H]dofetilide binding to the hERG channel and thallium ion flux through the channel (IC₅₀ value range: 2.1 – 6.6 μM). AZA1 did not block K⁺ current of the closely related EAG1 channel. Collectively, these data suggest that the AZAs physically block the K⁺ conductance pathway of hERG1 channels by occluding the cytoplasmic mouth of the open pore. Although the concentrations necessary to block hERG channels are relatively high, AZA-induced blockage may prove to contribute to the toxicological properties of the AZAs.

Keywords

azaspiracid (AZA); hERG; molecular target; voltage clamp; phycotoxin; potassium channel; channel binding assay; thallium flux assay

* CORRESPONDING AUTHOR: Michael J. Twiner Department of Natural Sciences University of Michigan-Dearborn 4901 Evergreen Rd Dearborn, MI USA 48128 office: (313) 593-5298 fax: (313) 593-4937 mtwiner@umd.umich.edu.

Introduction

Aspiracids (AZAs) are polyether toxins produced by toxigenic species of *Azadinium*^{1, 2} that can accumulate in shellfish and cause human illness.³ Although there have been no deaths associated with the AZA toxins, humans exposed to AZAs experience severe gastrointestinal illness.^{4, 5} Over the past decade, extensive progress has been made on elucidating the chemical structure of AZA and its various analogs. To date, over 20 naturally occurring analogs of AZA have been described,^{6, 7} but thus far only AZA1, AZA2, and AZA3 (Figure 1) appear to present a human health risk and are subject to food safety regulations.⁸ *In vivo* studies in mice exposed to AZA1 revealed severe effects such as deformation of intestinal epithelial villi^{9, 10} as well as damage to T and B lymphocytes, accumulation of fatty acid deposits in the liver, increased prevalence of lung tumors, and hyperplasia within the stomach lining.^{11, 12} *In vitro* studies have shown the AZAs to be highly cytotoxic causing a variety of cytoskeletal effects¹³⁻¹⁸ and stimulation of cAMP production and cytosolic calcium release.^{19, 20} In spinal cord neurons, AZA1 was shown to inhibit bioelectrical activity through a mechanism that was independent of voltage-gated sodium (Na⁺) or calcium (Ca²⁺) current.²¹ Recent findings suggest the AZAs cause apoptosis,^{13, 22, 23} although this toxin class may have multiple molecular targets^{13, 14} and also induce necrotic pathways concurrently.

To date, the mechanism(s) of action of the AZA toxin class has not been identified, but during a series of preliminary activity screening assays wherein AZA1 was tested towards various protein phosphatases, kinases, G-protein coupled receptors, and ion channels, there was an indication that AZA1 had an adverse effect on a member of the *ether-à-go-go* (EAG) K⁺ channel family. EAG K⁺ channels were first discovered in *Drosophila* where the *eag* mutant was associated with spontaneous repetitive axon firing in motor neurons.²⁴ It was later determined that *eag* encodes a K⁺ channel subunit²⁵ that functions to conduct a delayed rectifier K⁺ current.²⁶ A human homolog (*hEAG*) of *Drosophila eag* and a related gene (*hERG*, human *ether-à-go-go* related gene) were later discovered in a human hippocampus cDNA library.²⁷ hERG K⁺ channels are transcriptionally expressed in a broad array of cell/tissue types including heart (differentially expressed across the 4 chambers), brain, liver, kidney, breast, pancreas, and colon with the highest levels of expression in heart and brain tissue.²⁸ Expression is cell cycle dependent, involved in apoptosis,²⁹ and commonly up-regulated in cancerous cells.³⁰

The hERG (aka KCNH2) encodes the pore forming α subunit of the voltage-gated potassium channel Kv11.1.²⁷ The channel consists of four α subunits, each with six transmembrane domains (S1-S6) where S5 and S6 form the channel's central pore. In the heart, hERG proteins coassemble to form the channel that conducts the rapid delayed rectifier K⁺ current (I_{Kr}), which is critical for the repolarization phase of the cardiac action potential.³¹ Mutations in this channel have been associated with congenital long (and short) QT syndromes, characterized by prolonged (and shortened) ventricular repolarization and increased risk of fatal cardiac arrhythmia. The hERG channel has been shown to be the target for class III antiarrhythmic drugs such as dofetilide, which can reduce the risk of re-entrant arrhythmias by prolonging the action potential duration and refractory period without slowing conduction velocity in the myocardium. However, block of this channel by class III agents and numerous noncardiac drugs with poor predictability based on structure, can also cause excessive prolongation of QT intervals and induce arrhythmia ("acquired long QT syndrome"). Due to the wide spectrum of compounds that can block hERG channels and induce arrhythmia, drug regulatory agencies have issued recommendations for the evaluation of hERG activity in the early preclinical stages of drug development.

A variety of natural toxins are known to target hERG channels,³² including but not limited to scorpion venoms,³³ spider venoms,³⁴ sea anemone toxins,³⁵ and the algal toxins ciguatoxin,³⁶ and gambierol.³⁷ The aim of the current study was to examine the effects of AZAs on human ERG channels, providing the first mechanistic description of this interaction.

Materials and Methods

Toxin Isolation

The AZAs were isolated from cooked mussel tissue (*M. edulis*) collected in 2005 from Bruckless, Donegal, Ireland. The toxins were purified using a 7-step protocol as outlined by Kilcoyne et al.³⁸ and stored at -20 °C in methanol. Purity (>95%) was confirmed by LC-MS/MS and NMR spectroscopy. For experimental use, the AZAs were dried down under N₂ gas and resuspended in DMSO.

Mammalian cell voltage clamp protocols and data analysis

HEK-293 cells stably transfected with hERG cDNA (GenScript Inc., Piscataway, NJ, USA) were regularly subcultured in Dulbecco's Modified Eagle Medium supplemented with 10% fetal bovine serum and 200 µg/mL G418 antibiotic (cat. #G8168, Sigma-Aldrich, St. Louis, MO, USA). HEK-293 cells expressing hERG were plated in 35 mm dishes at least 24 h prior to the day of experiment and maintained at 37 °C/5% CO₂. The extracellular solution for whole cell patch clamp recordings was composed of (in mM): 137 NaCl; 1.2 MgCl₂; 5.4 KCl; 10 glucose; 10 HEPES; and 2 CaCl₂. pH was adjusted to 7.4 with NaOH. The osmolarity was adjusted to 305 mOsm with sucrose. The intracellular solution for whole cell patch clamp recordings was composed of (in mM): 140 KCl; 1 MgCl₂; 5 EGTA; 10 HEPES and 5 Na₂ATP. The pH was adjusted to 7.2 with KOH. The osmolarity was adjusted to 295 mOsm with sucrose.

For electrophysiology recordings, micropipettes were pulled from borosilicate glass that had a tip resistance of 3 - 5 MΩ when filled with intracellular solution. For each experiment, a single dish of cells was removed from the incubator, washed twice with room temperature (RT) extracellular solution and then placed on the microscope stage. A commercial patch clamp amplifier was used for the whole cell recordings. The tail currents were evoked at RT once every 30 s by a 3 s -50 mV repolarizing pulse following a 2 s +50 mV depolarizing test pulse. The holding potential was -80 mV and a 50 ms pulse to -50 mV preceded each test pulse and served as a baseline for calculating the amplitude of the peak tail current. Only stable cells with recording parameters above threshold were subjected to AZA exposure. The hERG channel currents were allowed to stabilize over a 3 min period in the presence of vehicle alone prior to AZA addition. The cells were kept in the test solution until the peak tail current was stable (< 5% change) for ~5 sweeps or for a maximum of 6 min, whichever came first. Criteria for acceptance of measurements were (i) whole-cell membrane resistance (R_m) was greater than 1,000 MΩ throughout the experiment, (ii) initial tail current was greater than 300 pA, (iii) series resistance value following establishment of whole-cell mode was less than 12 MΩ, and (iv) the leak current that the cell began with or developed over time was less than 10% of the ionic current magnitude (up to a maximum of 80 pA). The hERG channel antagonist terfenadine (cat. #T9652, Sigma-Aldrich, St. Louis, MO, USA) was used as a positive control. All test agent stock solutions were resuspended in DMSO and diluted in extracellular solution. DMSO additions never exceeded 0.3% vol./vol. which itself did not affect hERG currents (data not shown).

Voltage clamp data were recorded by Clampex (version 10.1) and data acquisition and analyses were performed using pCLAMP (version 10.1; Molecular Devices, CA, USA) and

Origin 8 (OriginLab Corp., MA, USA). Peak tail amplitudes were plotted as a function of the sweep number. Five peak tail current measurements at the steady state AZA addition were averaged and used as the control current amplitude. Four or five peak tail current measurements at the steady state after AZA addition were averaged and used as the remaining current amplitude after inhibition by AZA. The % inhibition of hERG channel due to AZA was calculated from the following equation: % inhibition = $(1 - (\text{remaining current amplitude} / (\text{control current amplitude}))) \times 100$. Unless stated differently, all data are presented as means \pm SEM of at least three independent experiments. IC₅₀ and 95% confidence interval determinations were calculated using four parameter, non-linear regression analysis (GraphPad Prism, ver. 5.0c, San Diego, CA, USA).

Heterologous expression of ERG channels in oocytes

Human *ERG1* cDNA (*KCNH2*; GenBank accession no. NP_000229) was cloned into the pSP64 oocyte expression vector. Two hERG channel mutants (Y652A and F656T), chosen because of the known sites that have been shown to attenuate block by many drugs,³⁹⁻⁴¹ were introduced using the QuikChange mutagenesis kit (Agilent Technologies, Santa Clara, CA, USA) and verified by DNA sequence analyses. *hERG1* plasmids were linearized with *EcoRI* and cRNA was prepared by *in vitro* transcription with mMessage mMachinE SP6 kit (Ambion, Austin, TX, USA) after linearization of plasmids with *EcoRI*. Human *EAG1* cDNA (*KCNH1*; GenBank accession no. AJ001366.1) cloned into psGEMHE oocyte expression vector was kindly provided by the late Dr. Dennis Wray. *hEAG1* plasmids were linearized by *NotI* and cRNA was prepared with the mMessage mMachinE T7 kit (Ambion, Austin, TX, USA). The concentration of cRNA was quantified using a RiboGreen assay (Life Technologies, Grand Island, NY, USA).

Oocyte isolation and cRNA injection

The procedures used to harvest oocytes from *Xenopus laevis* were approved by the University of Utah Institutional Animal Care and Use Committee. Briefly, frogs were anesthetized with 0.2% tricaine methane sulfonate before removal of ovarian lobes that were then manually dispersed with forceps, then treated for 90–120 min with 1 mg/mL of type II collagenase (Worthington Biochemical Corp., Lakewood, NJ, USA) in a Ca²⁺-free solution containing (in mM): 96 NaCl, 2 KCl, 1 MgCl₂, and 5 HEPES; pH 7.6. Stage IV and V oocytes were injected with ~5 ng (*hERG1*) or ~0.2 ng (*hEAG1*) wild-type (WT) or mutant cRNA per oocyte and incubated for 2-3 days at 18 °C in Barth's saline solution before use in voltage clamp experiments. Barth's solution contained (in mM): 88 NaCl, 2 KCl, 0.41 CaCl₂, 0.33 Ca(NO₃)₂, 1 MgSO₄, 2.4 NaHCO₃, 10 HEPES, 1 pyruvate, 50 mg/L gentamycin; pH 7.4.

Oocyte two-electrode voltage clamp protocols and data analysis

Ionic currents were recorded at 22–24 °C from single *Xenopus* oocytes using a standard two-microelectrode voltage clamp technique^{42, 43} using a GeneClamp 500 amplifier, and Digidata 1322A data acquisition system controlled by pCLAMP 8.2 software (Molecular Devices, Inc., Sunnyvale, CA, USA). Oocytes were placed in a static, small volume (75 μ L) recording chamber. The bathing solution contained (in mM): 98 NaCl, 2 KCl, 1 CaCl₂, 1 MgCl₂, 5 HEPES; pH 7.6. Agarose-cushion microelectrodes were fabricated as described⁴⁴ and had tip resistances of 0.4 – 0.6 M Ω when back-filled with 3 M KCl.

During an initial equilibration period, oocytes were voltage clamped to a holding potential of –80 mV, and 1-s pulses to a test potential (V_t) of 0 mV were applied every 10 s until current magnitude reached a steady-state level. The current-voltage ($I-V_t$) relationships for hERG1 or hEAG1 channels were determined by applying 2-s pulses to test potentials ranging from –70 to +40 mV in 10 mV increments. The holding potential was –80 mV and

tail currents were elicited at -70 mV. Conductance-voltage (G - V_t) relationships for hERG1 were determined by tail current analysis. Peak outward tail currents were normalized to their maximum value (at $+40$ mV) and plotted as a function of test potential. The resulting plot was fitted to a Boltzmann function (Eq. 1):

$$\frac{G}{G_{\max}} = \frac{1}{1 + \exp((V_t - V_{0.5})/k)} \quad (1)$$

where $V_{0.5}$ is the half-point of activation and k is the slope factor. The G - V relationship for hERG1 channels was determined by analysis of test pulse currents. The outward current at the end of 2-s pulses (I_{peak}) was divided by the electrical driving force, test voltage minus reversal potential ($V_t - E_{\text{rev}}$). The resulting relationship was fitted to a Boltzmann function and extrapolated to more positive potentials to estimate the maximum current (I_{max}) under control conditions. The G/G_{max} for each oocyte was then estimated as $I_{\text{peak}}/I_{\text{max}}$. The time-dependent decay of hERG1 tail currents elicited at -70 mV after activation pulses to $+40$ to 0 mV were fitted to a bi-exponential function (Levenberg-Marquardt method) to determine the time constants for channel deactivation.

After obtaining baseline recordings, a small aliquot of AZA1 stock solution ($500 \mu\text{M}$ in 10% DMSO) was added directly to the bathing solution to obtain the final desired toxin concentration. During the onset of AZA1 action, 1 s pulses to a V_t of 0 mV were applied every 10 s until a new steady-state current level was achieved. The I - V_t relationship protocol was then repeated in the presence of AZA1.

Off-line data analysis was performed with Clampfit 8.2 (Molecular Devices, CA, USA), Origin 8.5 (OriginLab, MA, USA) and Excel (Microsoft Corp., WA, USA) software. Data are expressed as mean \pm SEM (n = number of oocytes).

hERG channel binding assay

The hERG channel binding assay was performed as described by Huang et al.⁴⁵ Briefly, membranes were prepared from hERG-expressing HEK-293 cells and competition assays were performed in 96-well plates using [^3H]dofetilide (1.5 nM) in hERG binding buffer (hBB) containing (in mM): 135 NaCl, 5 KCl, 0.8 MgCl_2 , 10 HEPES, 10 glucose, 1 EGTA, and 0.01% BSA, pH 7.4. The AZA test compounds were diluted in hBB from $500 \mu\text{M}$ stock solutions in 10% DMSO / PBS (pH 7.4). Radioactivity retained on glass fiber filters was counted on a Perkin Elmer 1450 Microbeta Trilux plate counter and data are presented as disintegrations per minute (dpm). Dofetilide was used as a positive control. All data are presented as means \pm SEM of three replicate wells. IC_{50} and 95% confidence interval determinations were calculated using four parameter, non-linear regression analysis (GraphPad Prism, ver. 5.0c, CA, USA). Data (dpm per well) were also analyzed by non-linear regression, one-site saturation binding (GraphPad Prism) to obtain K_i values for each AZA analogue according to the Cheng-Prusoff equation.⁴⁶ An experimentally determined K_d value of 4.7 nM was used for [^3H]dofetilide.⁴⁵

Thallium flux assay

The thallium (Tl^+) flux assay was performed using the FluxOR Potassium Ion Channel Assay kit (cat. #F10016; Invitrogen, CA, USA) with modifications as outlined by Huang et al.⁴⁵ Briefly, hERG-expressing HEK-293 cells described above, were plated in 384-well plates, loaded with Tl^+ -sensitive FluxOR reagent, and incubated with AZA for 15 min prior to Tl^+ flux across hERG channels via stimulation with a K^+/Tl^+ -containing solution. Fluorescence intensity at 490/525 nm (ex./em.) of each well was simultaneously monitored using the FLIPR Tetra (MDS Analytical Technologies, Sunnyvale, CA, USA) with

ScreenWorks 2.9 software. Terfenadine was used as a positive control. Data are expressed as TI^+ flux as determined from the initial slope of the curve following hERG channel stimulation. All data are presented as means \pm SEM of three replicate wells. IC_{50} and 95% confidence interval determinations were calculated using four parameter, non-linear regression analysis (GraphPad Prism, ver. 5.0c, CA, USA).

Results

AZA1, AZA2, and AZA3 block hERG channel current in transfected mammalian cells

Voltage clamped HEK-293 cells stably expressing hERG channels were exposed to various concentrations of AZA1, AZA2, and AZA3 (0.064 - 1.9 μ M) and hERG currents were monitored while voltage was adjusted. Representative traces and replicated experimental data illustrate that hERG currents were inhibited by AZA1 in a concentration-dependent manner with a maximum inhibition of $79.5 \pm 1.8\%$ (mean \pm SEM, $n = 3$) elicited by 1.9 μ M AZA1 (Figure 2). As determined by patch clamp experiments, the AZA1 IC_{50} value was 0.84 μ M (Table 1). Similarly, AZA2 and AZA3 caused nearly identical concentration-dependent inhibition of hERG currents (Figure 2B; representative traces not shown). Maximal inhibition by AZA2 and AZA3 (1.9 μ M) was $87.3 \pm 0.95\%$ and $79.7 \pm 1.6\%$ with IC_{50} values of 0.64 μ M and 0.84 μ M; respectively. Relative potencies (relative to AZA1) are: AZA2 > AZA3 = AZA1. Terfenadine, a well-known inhibitor of hERG channels, elicited concentration-dependent inhibition of hERG currents (data not shown) with an IC_{50} of 0.019 μ M (Table 1).

AZA1 blocks hERG1 channels heterologously expressed in oocytes

The mechanisms of AZA1 induced inhibition of hERG1 channels were studied in greater detail using *Xenopus laevis* oocytes. WT hERG1 channel currents measured in oocytes were slightly less sensitive to AZA1 than currents in HEK-293 cells, but had similar inhibitory effects to those determined by binding studies in these cells described below. At a saturating concentration (10 μ M), AZA1 reduced the peak outward hERG1 current measured at -10 mV in oocytes to $19.0 \pm 2.4\%$ of control ($n = 6$). The onset of hERG1 channel block in oocytes by 10 μ M AZA1 developed exponentially with a time constant of 1.5 min (Figure 3A and B). The effect of 10 μ M AZA1 on the peak outward hERG1 currents (I_{peak}) elicited during pulses to a range of test voltages was determined. Steady-state changes in current magnitude were observed after 5 - 8 min. Representative currents are shown in Figure 3C (control) and 3D (5 min AZA1) and $I-V_t$ relationships are plotted in Figure 3E. I_{peak} was reduced at all potentials. AZA1 did not alter the voltage dependence of rectification (Figure 3C, open triangles), indicating that it had no effect on the voltage dependence of hERG channel inactivation. The voltage dependence of channel activation was determined by plotting the normalized peak tail currents measured at -70 mV as a function of V_t (Figure 3F). AZA1 reduced I_{tail} at all voltages and inhibited peak I_{tail} by $75 \pm 2\%$ ($n = 6$), but did not significantly alter the $V_{0.5}$ or slope factor of the $G-V_t$ curve determined using 2-s activating pulses. AZA1 caused a modest acceleration in the rate of current deactivation. At -70 mV, tail currents decayed with a bi-exponential time course with time constants of 249 ± 8 ms and 1003 ± 57 ms under control conditions and 205 ± 17 ms and 745 ± 44 ms in the presence of AZA1 ($n = 6$). The relative amplitude of the slow component of deactivation was slightly reduced by AZA1 from 0.80 ± 0.02 to 0.72 ± 0.02 .

Channel state dependent block by AZA1

To determine if AZA1 inhibition of hERG1 current depends on the state of the channel, we compared the time-course of currents recorded during single test pulses applied in the absence of AZA1 and again after a prolonged pulse-free period of AZA1 exposure. Control current was first activated with a very long (37.8 s) pulse to 0 mV (Figure 4). AZA1 (10

μM) was then added to the recording chamber and the oocyte was held at -70 mV without pulsing to keep channels in a closed state for 4 min. At the end of the 4 min incubation, a second long pulse to 0 mV was applied. Current traces for the two test pulses are superimposed in Figure 4A for the complete pulse, and in Figure 4B for the initial 1.35 s of the pulse. AZA1 had a minimal effect on current during the initial 0.5 s of the pulse; afterwards inhibition developed gradually during the long pulse and neared completion by the end of the pulse. To more clearly illustrate the time-dependent development of block by AZA1, the current trace recorded in the presence of AZA1 was divided by the control current trace and the resulting ratio ($I_{\text{AZA1}}/I_{\text{control}}$) plotted as a function of time in Figure 4C. The ratio $I_{\text{AZA1}}/I_{\text{control}}$ was initially 1.0 (indicating no closed state block), decayed with a bi-exponential time course and the extrapolated steady state ratio was 0.19. Thus, the amount of current was reduced to 19% of control during a single long pulse to 0 mV, similar to the average inhibition observed after 5-8 min of continual pulsing (Figure 4E). These findings suggest that AZA1 preferentially blocks the open state of hERG1 channels.

Mutation of F656 in S6 segment of hERG1 attenuates block by AZA1

Almost all compounds that block the open state of hERG1 channels appear to interact with a few residues in the S6 segment whose side chains face towards the central cavity.^{41, 47} Two of the most commonly recognized molecular determinants of hERG1 channel block are Phe656 and Tyr652 in S6; mutations in these residues have been shown to attenuate block by many drugs.³⁹⁻⁴¹ Therefore, we determined if mutation of either one of these residues affected block by AZA1. F656T hERG1 channels were insensitive to $10 \mu\text{M}$ AZA1 at test potentials negative to -20 mV (Figure 5A and B). At test potentials greater than -20 mV, currents were slightly inhibited (e.g., peak I_{tail} reduced by $7 \pm 1\%$; $n = 5$). Y652A hERG1 channel currents were inhibited by $10 \mu\text{M}$ AZA1 at all test potentials (Figure 5C) with $76 \pm 3\%$ ($n = 5$) block of peak I_{tail} (Figure 5D), similar to the block observed for WT hERG1 channels. AZA1 had no effect on the voltage dependence of F656T hERG1 channel activation (Figure 5B), but shifted the $V_{0.5}$ for activation of Y652A hERG1 channels by -5 mV (Figure 5D). Together the findings of reduced sensitivity of F656T hERG1 channels to block by AZA1 and the time-dependent inhibition of current following a pulse-free incubation with AZA1 (Figure 4) indicate that AZA1 is an open channel blocker.

AZA1 is a weak blocker of human EAG1 channels

To determine the channel specificity of AZA1, we examined the effect of $10 \mu\text{M}$ AZA1 on hEAG1 channels heterologously expressed in oocytes. AZA1 slightly reduced hEAG1 currents at all test potentials examined (Figure 6A-C). At a test potential of $+40$ mV, AZA1 blocked hEAG1 current by $15 \pm 0.8\%$ ($n = 4$). AZA1 did not alter the voltage dependence of channel activation (Figure 6D). Thus, AZA1 is a more potent blocker of hERG1 than hEAG1 K^+ channels.

AZA1, AZA2, and AZA3 bind to hERG channels

Membrane preparations from HEK-293 cells stably expressing hERG channels were used for binding assays. Various concentrations of AZA1, AZA2, and AZA3 (0.001 to $10 \mu\text{M}$) were tested and each AZA analog was found to inhibit binding of radiolabeled dofetilide, a known hERG inhibitor, in a concentration-dependent manner (Figure 7). The amount of bound [^3H]dofetilide is expressed as disintegrations per minute (dpm) (mean \pm SEM) per well. Relative to vehicle controls, hERG binding by AZA1, AZA2, and AZA3 ($10 \mu\text{M}$) was reduced to $19.7 \pm 1.4\%$ ($n = 2$), $22.3 \pm 1.0\%$ ($n = 3$), and $29.3 \pm 1.6\%$ ($n = 3$) with IC_{50} values of $2.1 \mu\text{M}$, $2.6 \mu\text{M}$, and $6.6 \mu\text{M}$; respectively (Table 1). Similarly, K_i values (with 95% confidence intervals) were 2.9 ($1.3 - 6.6$) μM , 3.6 ($1.9 - 6.9$) μM , and 8.3 ($3.5 - 20$) μM , respectively. As such, there were no statistical differences in the potencies of the three analogues (AZA1 = AZA2 = AZA3). Dofetilide, a well-known inhibitor of hERG channels,

elicited concentration-dependent inhibition of hERG binding (data not shown) with an IC_{50} of 8.8 nM (Table 1).

AZA1, AZA2, and AZA3 inhibit thallium flux through the hERG channel

The flux of thallium (Tl^+) through hERG channels was monitored in the presence and absence of AZA1, AZA2, and AZA3 (0.001 to 30 μ M). Each analog of AZA inhibited the flux of thallium in a concentration-dependent manner (Figure 8). All data (mean \pm SEM, $n = 3$) are expressed as the Tl^+ flux as determined from the initial slope of the curve following the addition of stimulation solution. Relative to vehicle controls, thallium flux via the hERG was reduced by AZA1, AZA2, and AZA3 (30 μ M) to $10.7 \pm 0.56\%$, $9.6 \pm 0.79\%$, and $16.6 \pm 0.50\%$ with IC_{50} values of 4.2 μ M, 5.1 μ M, and 6.2 μ M; respectively (Table 1). As such, there were no significant potency differences between the AZA analogues (AZA1 = AZA2 = AZA3). Terfenadine elicited a concentration-dependent inhibition of Tl^+ flux (data not shown) with an IC_{50} of 8.4 μ M (Table 1).

Discussion

Azaspiracids are potent algal toxins that have resulted in multiple human intoxication events in Europe and the United States.^{4, 5} Due to the growing food safety concerns related to this human health threat, many investigators have focused on elucidation of the molecular target(s) for this toxin class. However, despite these efforts, no specific target has been identified. For the first time, we present conclusive evidence that the AZA toxins are a new class of hERG K^+ channel inhibitors.

A wide range of drugs (and toxins) have been shown to inhibit hERG1 currents and in-depth studies indicate that most of these compounds block K^+ conductance by binding to a canonical site and plugging the central cavity that is formed by the four S6 segments of the homotetrameric channel.⁴⁸ The side-chains of two aromatic residues (Y652 and F656) located in each of the four S6 segments of hERG1 face towards the central cavity and are commonly involved with hydrophobic and/or π -stacking interactions with drugs that bind to the central cavity.^{39-41, 47, 49} Similar to AZA1 ($C_{47}H_{71}NO_{12}$), the macrolide antibiotic erythromycin ($C_{37}H_{67}NO_{13}$) also blocks hERG1 rapidly in an open-state dependent manner and analysis of mutant channels and molecular modeling indicate that it interacts with phenylalanine residue at position 656 but not with tyrosine residue at position 652.⁵⁰ AZA1 and erythromycin have molecular weights of 842 and 733, respectively and are much larger than the vast majority of drugs known to block hERG1 channels. Although Y652 is located only a single helical turn above F656 on S6, it is positioned further into the central cavity and may be beyond reach of compounds as large as AZA1 and erythromycin. Thus, while both AZA1 and erythromycin are open state-dependent blockers of hERG1, it seems their large size precludes their access into the deep interior of the central cavity. We propose that AZA1 physically blocks the K^+ conductance pathway of hERG1 channels by occluding the cytoplasmic mouth of the open pore. Pore block at this site might also explain why AZA1 does not appreciably alter the kinetics or voltage dependence of hERG1 channel gating. Collectively, these findings are consistent with our previous patch-clamp study using spinal cord neuronal networks wherein we concluded that AZA1 inhibited bioelectrical activity through a mechanism that was independent of voltage-gated sodium (Na^+) or calcium (Ca^{2+}) currents.²¹ However, it should be noted that bioelectrical activity was inhibited by low nanomolar concentrations of AZA1 whereas in the present study, much higher concentrations were necessary (i.e., micromolar).

EAG1 channels are closely related to ERG1 channels and yet are much less sensitive to block by AZA1. This difference in potency has been noted for most well studied hERG1 blockers and has been attributed at least in part to the orientation of the two aromatic

residues in the S6 segment of the two channels.⁵¹ Perhaps Phe468 in hEAG1 (equivalent to Phe656 in hERG1) is not positioned for optimum hydrophobic interaction with AZA1 when the channels are in the open state.

Relative to AZA1, AZA2 is methylated at the C8 position (8-methyl-azaspiracid) whereas AZA3 is demethylated at the C22 position (22-demethyl-azaspiracid) (Figure 1). Despite the methylation differences of these three AZA analogues, there does not appear to be much difference in relative potencies towards hERG K⁺ channel inhibition. Each AZA analogue was capable of inhibiting hERG K⁺ channel current in transfected HEK-293 cells with IC₅₀ values ranging between 0.64 and 0.84 μM. AZA2 was slightly more potent but the potencies of AZA3 and AZA1 were not different. However, this same trend in relative potency was not observed via hERG channel binding (K_i values between 2.9 and 8.3 μM) and thallium flux where all AZA analogues were found to be of the same relative potency. In contrast, it has been shown that there are very distinctive structure-activity relationships with respect to the cytotoxic potencies of these same AZA analogues at much smaller concentrations (i.e., low nanomolar). AZA2 and AZA3 have been shown to be 8.3- and 4.5-fold more potent than AZA1; respectively.¹⁴ These potency trends have also been corroborated *in vivo* via mouse lethality,^{52, 53} which have formed the basis for calculating the toxic equivalence factors (TEFs) currently used by the European Union for food safety regulation (1.8 for AZA2 and 1.4 for AZA3).⁸

AZAs are known to be highly potent cytotoxic agents to all cell types tested^{15, 54} and have been shown to induce apoptosis.²² Similarly, many hERG channel inhibitors are also known inducers of apoptosis²⁹ and can cause cytotoxicity towards a wide variety of cell lines.^{55, 56} Although cardiomyocytes and neurons are most sensitive, the broad distribution of hERG channels across many cell/tissue types likely plays a role in mediating this cytotoxic response. When administered via intraperitoneal injection to rodents, AZAs can cause a variety of neurotoxic, immunotoxic, and hepatotoxic effects that can result in death.^{52, 53, 57} In fact, the very first AZA studies used contaminated shellfish extracts that were injected into mice and caused a 'neurotoxin-like' response followed by death.^{58, 59} This response quite feasibly could have been via potassium channel inhibition.

In vitro, AZAs have been shown to directly enter into cells.⁶⁰ When administered orally, AZAs are systemically distributed^{9, 10} and can cause severe gastrointestinal degradation followed by a variety of other effects including hepatotoxicity and immunotoxicity.^{11, 12} Many of the other open channel blockers of hERG (i.e., methanesulfonanilides such as E-4031, MK-499, and dofetilide) can have a wide spectrum of toxicological effects *in vivo*, but generally do not have a history of gastrointestinal side effects^{61, 62} despite the presence of hERG channels in intestinal epithelial cells. *In vivo* exposure to mechanistically similar hERG channel blocking compounds such as erythromycin can have profound hepatotoxic effects⁶³ not unlike those induced by AZAs but commonly have their most dramatic effects on the heart, causing prolongation of cardiac action potentials,⁶⁴ which may lead to a potentially lethal form of cardiac arrhythmia called torsades-de-pointes. During a recent mini-pig feeding study, animals were acutely administered AZA-contaminated feed (200 μg AZA_{total}/kg) and monitored over a 24 h period. Despite an absence of overt symptoms, there were histological indications of gastrointestinal perturbations and coincident with peak AZA_{total} blood concentrations (ca. 3.2 nM at 4 h) peripheral lymphocyte differential gene expression using DNA microarrays were suggestive of a strong inflammatory response including markers of cardiomyopathy (unpubl. data). These preliminary findings provide the first physiological linkage between potassium channel inhibition and AZA toxicity. As such, future *in vivo* studies testing AZAs should assess potential cardiotoxic effects of these toxins (i.e., electrocardiogram, molecular markers, etc.).

A mechanism of action for the AZA toxin class has been sought for many years by multiple investigators. Although we have confirmed that AZAs are low affinity hERG potassium channel inhibitors, it is almost certain that the AZAs have other molecular targets as discussed previously.^{13, 14, 19} There are discrepancies between the concentrations and relative potencies of the AZA analogues necessary to cause cytotoxicity (sub- to low-nanomolar with AZA2 > AZA3 > AZA1) and those that are needed to inhibit hERG channel current (640 nM with AZA2 > AZA1 = AZA3). Similarly, *in vivo* toxic doses tend to be much lower for AZAs (500 g/kg)^{9, 10, 52, 53} relative to many of the other known hERG channel inhibitors (> 5 mg/kg). Finally, our previous study has shown that AZA1 is highly cytotoxic to wild-type HEK-293 cells (EC₅₀ values range between 2.5 and 4.6 nM)¹⁵ that do not have hERG K⁺ channels. As such, these discrepancies suggest that another molecular target(s) may be responsible for the cytotoxic effects of the AZAs.

The effects of long-term exposure of AZAs to human health are unknown. AZA1 has been shown to be a possible carcinogen in rodents¹¹ and a teratogen to developing fish where we specifically noted dose-dependent bradycardia⁶⁵ which has been demonstrated for several other hERG blockers⁶⁶ including erythromycin⁶⁷. It is conceivable that humans consuming AZAs via contaminated shellfish may be at risk for teratogenicity and/or torsades-de-pointes; however, targeted diagnostic evaluation of teratogenicity and cardiac function will be required to confirm such a response.

Conclusions

For the first time we have conclusively identified the hERG channel as a molecular target for the AZA toxins. Through the use of voltage clamp, channel binding studies, and ion flux assays, we have demonstrated that AZA1, AZA2, and AZA3 bind to and block potassium current through hERG channels. AZA1 was shown to be an open state-dependent blocker of hERG1 that interacts with F656 within the S6 transmembrane domain that forms the channel's central pore. We propose that AZA1 physically blocks the K⁺ conductance pathway of hERG1 channels by occluding the cytoplasmic mouth of the open pore. Although AZAs block with low affinity, these findings set the stage for future studies assessing the involvement of hERG channel blocking in AZA-induced toxicity. Furthermore, these findings may facilitate the identification of other molecular targets and the development of a functional channel binding bioassay that will be useful for rapid, high-throughput screening assays of naturally contaminated seafood.

Acknowledgments

Special thanks go to Jane Kilcoyne, Chris Miles, Philipp Hess, Adela Keogh, Conor Duffy, Ger Clancy, Pearse McCarron, Nils Rehmman, Daniel o'Driscoll, and Michael Quilliam for AZA purification, Vaman Naik for assistance with Origin software, and the NIMH-Psychoactive Drug Screening Program Contract. This publication does not constitute an endorsement of any commercial product or intend to be an opinion beyond scientific or other results obtained by the National Oceanic and Atmospheric Administration (NOAA). No reference shall be made to NOAA, or this publication furnished by NOAA, to any advertising or sales promotion which would indicate or imply that NOAA recommends or endorses any proprietary product mentioned herein, or which has as its purpose an interest to cause the advertised product to be used or purchased because of this publication.

Funding Support

This work (Grant-Aid Agreement No. 221117) was supported by the *Sea Change* strategy with the support of the Marine Institute and the Marine Research Sub-programme of the National Development Plan 2007–2013, co-financed under the European Regional Development Fund; the National Institutes of Health/National Heart, Lung and Blood Institute grant (R01 HL55236); and a UM-D Office of Research and Sponsored Programs Faculty Initiation and Seed Grant and the NIMH Psychoactive Drug Screening Program.

Abbreviations

hERG	human <i>ether-a-go-go-related gene</i>
AZA	azaspiracid
hBB	hERG binding buffer
DMSO	dimethyl sulfoxide
PBS	phosphate buffered saline
dpm	disintegrations per minute
CI	confidence interval
IC₅₀	50% inhibitory concentration
LC-MS/MS	liquid chromatography-mass spectrometry/mass spectrometry
I_{Kr}	rapid delayed rectifier potassium current

References

1. Krock B, Tillmann U, John U, Cembella AD. Characterization of azaspiracids in plankton size-fractions and isolation of an azaspiracid-producing dinoflagellate from the North Sea. *Harmful Algae*. 2009; 8:254–263.
2. Tillmann U, Elbrächter M, Krock B, John U, Cembella A. *Azadinium spinosum* gen. et sp. nov. (Dinophyceae) identified as a primary producer of azaspiracid toxins. *Eur. J. Phycol.* 2009; 44:63–79.
3. Hess, P.; McCarron, P.; Rehmann, N.; Kilcoyne, J.; McMahon, T.; Ryan, G.; Ryan, PM.; Twiner, MJ.; Doucette, GJ.; Satake, M.; Ito, E.; Yasumoto, T. Final project report ASTOX (ST/02/02). Marine Institute – Marine Environment & Health Series; Rinville, Co. Galway: 2007. Isolation and purification of azaspiracids from naturally contaminated materials, and evaluation of their toxicological effects.; p. 129
4. Twiner MJ, Rehmann N, Hess P, Doucette GJ. Azaspiracid shellfish poisoning: A review on the chemistry, ecology, and toxicology with an emphasis on human health impacts. *Mar. Drugs*. 2008; 6:39–72. [PubMed: 18728760]
5. Furey A, O'Doherty S, O'Callaghan K, Lehane M, James KJ. Azaspiracid poisoning (AZP) toxins in shellfish: Toxicological and health considerations. *Toxicon*. 2010; 56:173–190. [PubMed: 20026101]
6. James KJ, Sierra MD, Lehane M, Braña Magdalena A, Furey A. Detection of five new hydroxyl analogues of azaspiracids in shellfish using multiple tandem mass spectrometry. *Toxicon*. 2003; 41:277–283. [PubMed: 12565749]
7. Rehmann N, Hess P, Quilliam M. Discovery of new analogs of the marine biotoxin azaspiracid in blue mussels (*Mytilus edulis*) by ultra-performance liquid chromatography/tandem mass spectrometry. *Rapid Commun. Mass Spectrom.* 2008; 22:549–558. [PubMed: 18228242]
8. EFSA. Marine biotoxins in shellfish – Azaspiracid group: Scientific Opinion of the Panel on Contaminants in the Food chain. *The EFSA Journal*. 2008; 723:1–52.
9. Aune T, Espenes A, Aasen JAB, Quilliam MA, Hess P, Larsen S. Study of possible combined toxic effects of azaspiracid-1 and okadaic acid in mice via the oral route. *Toxicon*. 2012; 60:895–906. [PubMed: 22750012]
10. Aasen JAB, Espenes A, Hess P, Aune T. Sub-lethal dosing of azaspiracid-1 in female NMRI mice. *Toxicon*. 2010; 56:1419–1425. [PubMed: 20800607]
11. Ito E, Satake M, Ofuji K, Higashi M, Harigaya K, McMahon T, Yasumoto T. Chronic effects in mice caused by oral administration of sublethal doses of azaspiracid, a new marine toxin isolated from mussels. *Toxicon*. 2002; 40:193–203. [PubMed: 11689241]

12. Ito E, Satake M, Ofuji K, Kurita N, McMahon T, James K, Yasumoto T. Multiple organ damage caused by a new toxin azaspiracid, isolated from mussels produced in Ireland. *Toxicol.* 2000; 38:917–930. [PubMed: 10728830]
13. Cao Z, LePage KT, Frederick MO, Nicolaou KC, Murray TF. Involvement of caspase activation in azaspiracid-induced neurotoxicity in neocortical neurons. *Toxicol. Sci.* 2010; 114:323–334. [PubMed: 20047973]
14. Twiner MJ, El-Ladki R, Kilcoyne J, Doucette GJ. Comparative effects of the marine algal toxins azaspiracid-1, -2, and -3 on Jurkat T lymphocyte cells. *Chem. Res. Toxicol.* 2012; 25:747–754. [PubMed: 22375692]
15. Twiner MJ, Hess P, Bottein Dechraoui M-Y, McMahon T, Samons MS, Satake M, Yasumoto T, Ramsdell JS, Doucette GJ. Cytotoxic and cytoskeletal effects of azaspiracid-1 on mammalian cell lines. *Toxicol.* 2005; 45:891–900. [PubMed: 15904684]
16. Vale C, Nicolaou KC, Frederick MO, Gomez-Limia B, Alfonso A, Vieytes MR, Botana LM. Effects of azaspiracid-1, a potent cytotoxic agent, on primary neuronal cultures. A structure-activity relationship study. *J. Med. Chem.* 2007; 50:356–363. [PubMed: 17228878]
17. Vilariño N, Nicolaou KC, Frederick MO, Cagide E, Ares IR, Louzao MC, Vieytes MR, Botana LM. Cell growth inhibition and actin cytoskeleton disorganization induced by azaspiracid-1 structure-activity studies. *Chem. Res. Toxicol.* 2006; 19:1459–1466. [PubMed: 17112233]
18. Vilariño N. Marine toxins and the cytoskeleton: azaspiracids. *FEBS J.* 2008; 275:6075–6081. [PubMed: 19016861]
19. Roman Y, Alfonso A, Louzao MC, de la Rosa LA, Leira F, Vieites JM, Vieytes MR, Ofuji K, Satake M, Yasumoto T, Botana LM. Azaspiracid-1, a potent, nonapoptotic new phycotoxin with several cell targets. *Cell. Signalling.* 2002; 14:703–716. [PubMed: 12020771]
20. Roman Y, Alfonso A, Vieytes MR, Ofuji K, Satake M, Yasumoto T, Botana LM. Effects of azaspiracids 2 and 3 on intracellular cAMP, $[Ca^{2+}]_i$, and pH. *Chem. Res. Toxicol.* 2004; 17:1338–1349. [PubMed: 15487894]
21. Kulagina KV, Twiner MJ, Hess P, McMahon T, Satake M, Yasumoto T, Ramsdell JS, Doucette GJ, Ma W, O'Shaughnessy TJ. Azaspiracid-1 inhibits bioelectrical activity of spinal cord neuronal networks. *Toxicol.* 2006; 47:766–773. [PubMed: 16626774]
22. Twiner MJ, Hanagriff JC, Butler SC, Madhkoor AK, Doucette GJ. Induction of apoptosis pathways in several cell lines following exposure to the marine algal toxin azaspiracid-1. *Chem. Res. Toxicol.* 2012; 25:1493–1501. [PubMed: 22725096]
23. Vilariño N, Nicolaou KC, Frederick MO, Vieytes MR, Botana LM. Irreversible cytoskeletal disarrangement is independent of caspase activation during *in vitro* azaspiracid toxicity in human neuroblastoma cells. *Biochem. Pharmacol.* 2007; 74:327–335. [PubMed: 17485074]
24. Ganetzky B, Wu CF. Neurogenetic analysis of potassium currents in *Drosophila*: synergistic effects on neuromuscular transmission in double mutants. *J. Neurogenet.* 1983; 1:17–28. [PubMed: 6100303]
25. Warmke J, Drysdale R, Ganetzky B. A distinct potassium channel polypeptide encoded by the *Drosophila* eag locus. *Science.* 1991; 252:1560–1562. [PubMed: 1840699]
26. Bruggemann A, Pardo LA, Stuhmer W, Pongs O. Ether-a-go-go encodes a voltage-gated channel permeable to K^+ and Ca^{2+} and modulated by cAMP. *Nature.* 1993; 365:445–448. [PubMed: 7692301]
27. Warmke JW, Ganetzky B. A family of potassium channel genes related to EAG in *Drosophila* and mammals. *Proc Natl Acad Sci USA.* 1994; 91:3438–3442. [PubMed: 8159766]
28. Luo X, Xiao J, Lin H, Lu Y, Yang B, Wang Z. Genomic structure, transcriptional control, and tissue distribution of HERG1 and KCNQ1 genes. *Am. J. Physiol. Heart Circ. Physiol.* 2008; 294:H1371–H1380.
29. Jehle J, Schweizer P, Katus H, Thomas D. Novel roles for hERG K^+ channels in cell proliferation and apoptosis. *Cell Death Dis.* 2011; 2:e193. [PubMed: 21850047]
30. Pardo LA, del Camino D, Sanchez A, Alves F, Bruggemann A, Beckh S, Stuhmer W. Oncogenic potential of EAG K^+ channels. *Embo J.* 1999; 18:5540–5547. [PubMed: 10523298]

31. Sanguinetti MC, Jiang C, Curran ME, Keating MT. A mechanistic link between an inherited and an acquired cardiac arrhythmia: hERG encodes the I_{K_r} potassium channel. *Cell*. 1995; 81:299–307. [PubMed: 7736582]
32. Jiménez-Vargas, JM.; Restano-Cassulini, R.; Possani, LD. Toxin modulators and blockers of hERG K^+ channels.. *Toxicon*: in press
33. Pardo-Lopez L, Zhang M, Liu J, Jiang M, Possani LD, Tseng GN. Mapping the binding site of a human ether-a-go-go-related gene-specific peptide toxin (ErgTx) to the channel's outer vestibule. *J Biol Chem*. 2002; 277:16403–16411. [PubMed: 11864985]
34. Redaelli E, Cassulini RR, Silva DF, Clement H, Schiavon E, Zamudio FZ, Odell G, Arcangeli A, Clare JJ, Alagon A, de la Vega RCR, Possani LD, Wanke E. Target promiscuity and heterogeneous effects of tarantula venom peptides affecting Na^+ and K^+ ion channels. *J. Biol. Chem*. 2010; 285:4130–4142. [PubMed: 19955179]
35. Zhang M, Liu XS, Diochot S, Lazdunski M, Tseng GN. APETx1 from sea anemone *Anthopleura elegantissima* is a gating modifier peptide toxin of the human ether-a-go-go-related potassium channel. *Mol Pharmacol*. 2007; 72:259–268. [PubMed: 17473056]
36. Birinyi-Strachan LC, Gunning SJ, Lewis RJ, Nicholson GM. Block of voltage-gated potassium channels by Pacific ciguatoxin-1 contributes to increased neuronal excitability in rat sensory neurons. *Toxicol. Appl. Pharm*. 2005; 204:175–186.
37. Alonso E, Fuwa H, Vale C, Suga Y, Goto T, Konno Y, Sasaki M, LaFerla FM, Vieytes MR, Giménez-Llort L, Botana LM. Design and synthesis of skeletal analogues of gambierol: Attenuation of amyloid- β and Tau pathology with voltage-gated potassium channel and N-methyl-d-aspartate receptor implications. *J. Am. Chem. Soc*. 2012; 134:7467–7479. [PubMed: 22475455]
38. Kilcoyne J, Keogh A, Clancy G, Le Blanc P, Burton I, Quilliam M, Hess P, Miles CO. Improved isolation procedure for azaspiracids from shellfish, structural elucidation of azaspiracid-6, and stability studies. *J. Agric. Food Chem*. 2012; 60:2447–2455. [PubMed: 22329755]
39. Fernandez D, Ghanta A, Kauffman GW, Sanguinetti MC. Physicochemical features of the hERG channel drug binding site. *J. Biol. Chem*. 2004; 279:10120–10127. [PubMed: 14699101]
40. Lees-Miller JP, Duan Y, Teng GQ, Duff HJ. Molecular determinant of high-affinity dofetilide binding to HERG1 expressed in *Xenopus* oocytes: involvement of S6 sites. *Mol Pharmacol*. 2000; 57:367–374. [PubMed: 10648647]
41. Mitcheson JS, Chen J, Lin M, Culberson C, Sanguinetti MC. A structural basis for drug-induced long QT syndrome. *Proc. Natl. Acad. Sci. USA*. 2000; 97:12329–12333. [PubMed: 11005845]
42. Goldin AL. Expression of ion channels by injection of mRNA into *Xenopus oocytes*. *Methods Cell. Biol*. 1991; 36:487–509. [PubMed: 1725803]
43. Stuhmer W. Electrophysiological recording from *Xenopus oocytes*. *Methods Enzymol*. 1992; 207:319–339. [PubMed: 1382188]
44. Schreibmayer W, Lester HA, Dascal N. Voltage clamping of *Xenopus laevis* oocytes utilizing agarose-cushion electrodes. *Pflugers Arch*. 1994; 426:453–458. [PubMed: 7517034]
45. Huang X-P, Mangano T, Hufeisen S, Setola V, Roth BL. Identification of human ether-a-go-go related gene modulators by three screening platforms in an academic drug-discovery setting. *Assay Drug Dev Technol*. 2010; 8:727–742. [PubMed: 21158687]
46. Yung-Chi C, Prusoff WH. Relationship between the inhibition constant (K_I) and the concentration of inhibitor which causes 50 per cent inhibition (I_{50}) of an enzymatic reaction. *Biochem. Pharmacol*. 1973; 22:3099–3108. [PubMed: 4202581]
47. Sanguinetti MC, Mitcheson JS. Predicting drug-hERG channel interactions that cause acquired long QT syndrome. *Trends Pharmacol. Sci*. 2005; 26:119–124. [PubMed: 15749156]
48. Sanguinetti MC, Tristani-Firouzi M. hERG potassium channels and cardiac arrhythmia. *Nature*. 2006; 440:463–469. [PubMed: 16554806]
49. Kamiya K, Niwa R, Morishima M, Honjo H, Sanguinetti MC. Molecular determinants of hERG channel block by terfenadine and cisapride. *J Pharmacol Sci*. 2008; 108:301–307. [PubMed: 18987434]
50. Duncan RS, Ridley JM, Dempsey CE, Leishman DJ, Leaney JL, Hancox JC, Witchel HJ. Erythromycin block of the HERG K^+ channel: accessibility to F656 and Y652. *Biochem Biophys Res Commun*. 2006; 341:500–506. [PubMed: 16446155]

51. Chen J, Seeböhm G, Sanguinetti MC. Position of aromatic residues in the S6 domain, not inactivation, dictates cisapride sensitivity of HERG and eag potassium channels. *Proc Natl Acad Sci USA*. 2002; 99:12461–12466. [PubMed: 12209010]
52. Ofuji K, Satake M, McMahon T, Silke J, James KJ, Naoki H, Oshima Y, Yasumoto T. Two analogs of azaspiracid isolated from mussels, *Mytilus edulis*, involved in human intoxication in Ireland. *Nat. Toxins*. 1999; 7:99–102. [PubMed: 10647511]
53. Satake M, Ofuji K, Naoki H, James KJ, Furey A, McMahon T, Silke J, Yasumoto T. Azaspiracid, a new marine toxin having unique spiro ring assemblies, isolated from Irish mussels, *Mytilus edulis*. *J. Am. Chem. Soc*. 1998; 120:9967–9968.
54. Twiner MJ, Ryan JC, Morey JS, Smith KJ, Hammad SM, Van Dolah FM, Hess P, McMahon T, Satake M, Yasumoto T, Doucette GJ. Transcriptional profiling and inhibition of cholesterol biosynthesis in human lymphocyte T cells by the marine toxin azaspiracid. *Genomics*. 2008; 91:289–300. [PubMed: 18191373]
55. Waldhauser KM, Brecht K, Hebeisen S, Ha HR, Konrad D, Bur D, Krähenbühl S. Interaction with the hERG channel and cytotoxicity of amiodarone and amiodarone analogues. *Br. J. Pharmacol*. 2008; 155:585–595. [PubMed: 18604229]
56. Viluksela M, Vainio PJ, Tuominen RK. Cytotoxicity of macrolide antibiotics in a cultured human liver cell line Matti Viluksela. *J. Antimicrob. Chemother*. 1996; 38:465–473. [PubMed: 8889721]
57. Ito, E.; Terao, K.; McMahon, T.; Silke, J.; Yasumoto, T. Acute pathological changes in mice caused by crude extracts of novel toxins isolated from Irish mussels. In: Reguera, B.; Blanco, J.; Fernandez, ML.; Wyatt, T., editors. *Harmful Algae*. Xunta de Galicia and Intergovernmental Oceanographic Commission of UNESCO; Santiago de Compostela: 1998. p. 588-589.
58. McMahon T, Silke J. Winter toxicity of unknown aetiology in mussels. *Harmful Algae News*. 1996; 14:2.
59. McMahon T, Silke J. Re-occurrence of winter toxicity. *Harmful Algae News*. 1998; 17:12.
60. Vilariño N, Nicolaou KC, Frederick MO, Cagide E, Alfonso C, Alonso E, Vieytes MR, Botana LM. Azaspiracid substituent at C1 is relevant to *in vitro* toxicity. *Chem. Res. Toxicol*. 2008; 21:1823–1831. [PubMed: 18707138]
61. Camm J. Antiarrhythmic drugs for the maintenance of sinus rhythm: Risks and benefits. *Int. J. Cardiol*. 2012; 155:362–371. [PubMed: 21708411]
62. Torp-Pedersen C, Møller M, Bloch-Thomsen PE, Køber L, Sandøe E, Egstrup K, Agner E, Carlsen J, Videbæk J, Marchant B, Camm AJ. Dofetilide in patients with congestive heart failure and left ventricular dysfunction. *N Engl J Med*. 1999; 341:857–865. [PubMed: 10486417]
63. Viluksela M, Hanhijärvi H, Husband RFA, Kosma V-M, Collan Y, Männistö PT. Comparative liver toxicity of various erythromycin derivatives in animals. *J. Antimicrob. Chemother*. 1988; 21:9–27. [PubMed: 3391880]
64. Yap Y, Camm J. Risk of torsades de pointes with non-cardiac drugs. *Brit. Med. J*. 2000; 320:1158–1159. [PubMed: 10784527]
65. Colman JR, Twiner MJ, Hess P, McMahon T, Satake M, Yasumoto T, Doucette GJ, Ramsdell JS. Teratogenic effects of azaspiracid-1 identified by microinjection of Japanese medaka (*Oryzias latipes*) embryos. *Toxicol*. 2005; 45:881–890. [PubMed: 15904683]
66. Karlsson M, Danielsson BR, Nilsson MF, Danielsson C, Webster WS. New proposals for testing drugs with IKr-blocking activity to determine their teratogenic potential. *Curr. Pharmaceut. Design*. 2007; 13:2979–2988.
67. Kallen B, Otterblad Olausson P, Danielsson B. Is erythromycin therapy teratogenic in humans? *Reprod. Toxicol*. 2005; 20:209–214. [PubMed: 15907655]

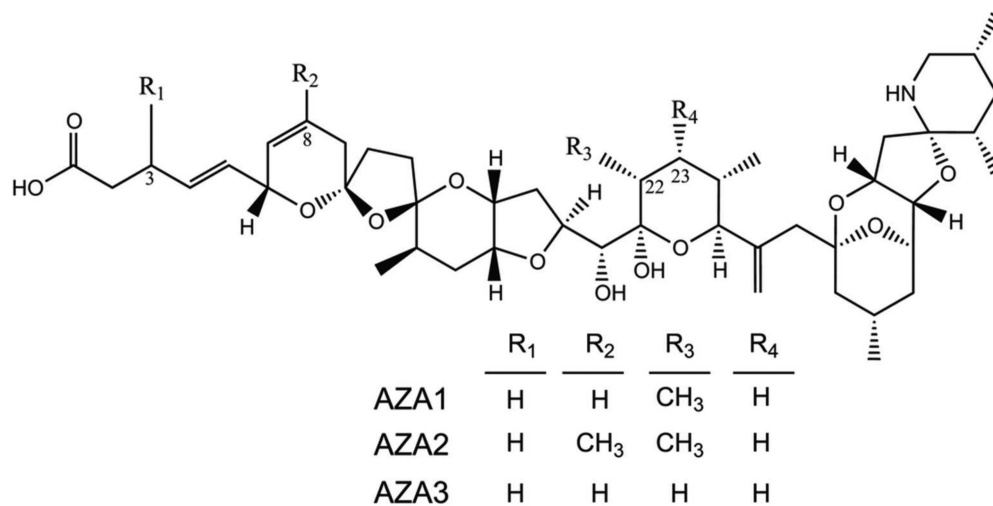


Figure 1.
Chemical structures of AZA1, AZA2, and AZA3.

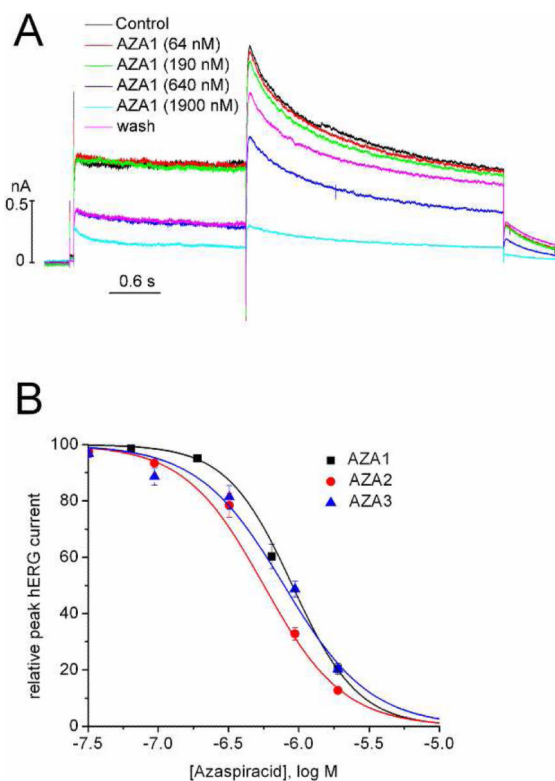


Figure 2. AZAs block hERG1 channels expressed in HEK-293 cells. (A) Representative patch clamp traces of potassium ion current through hERG channels stably expressed in HEK-293 cells in the presence of various concentrations of AZA1. (B) Concentration-dependent inhibition of potassium ion current through hERG channels by AZA1, AZA2, and AZA3. Data (mean \pm SEM; n=3) were normalized to the control (DMSO vehicle) and analyzed using non-linear sigmoidal dose-response (variable slope). Terfenadine was used as a positive control (data not shown). Calculated IC_{50} values are shown in Table 1.

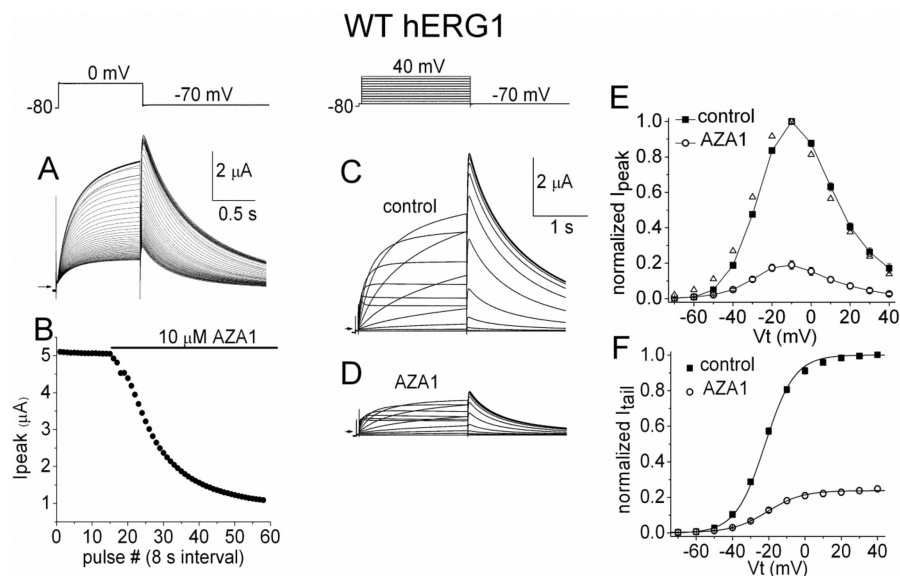


Figure 3. AZA1 blocks hERG1 channels expressed in *Xenopus* oocytes in a voltage-independent manner. (A) Voltage clamp protocol (upper panel) and currents (lower panel) recorded during repetitive pulsing to 0 mV. Pulse duration was 1 s and the interpulse interval was 8 s. The initial 15 pulses were recorded in the absence of toxin; the remaining traces illustrate the gradual reduction in current amplitude during the onset of channel block by 10 μ M AZA1. (B) Peak outward current at the end of the 1-s pulse (I_{peak}) plotted as a function of time after addition of AZA1. The onset of block developed exponentially with a time constant (τ_{onset}) of 1.5 min. (C) and (D) Voltage clamp protocol (upper panel) and current traces (middle and bottom panels) recorded during control conditions (C) and 7 min after addition of 10 μ M AZA1 (D) to the recording chamber. (E) Effect of AZA1 on I - V_t relationship ($n = 6$). The AZA1 current amplitudes were multiplied by 5.274 and replotted (open triangles) to facilitate comparison of the voltage-dependence of the I - V relationships between control and AZA1 currents. AZA1 did not alter the voltage dependence of rectification, indicating that it had no effect on the voltage dependence of hERG channel inactivation. (F) Effect of 10 μ M AZA1 on the G - V_t relationship. Normalized I_{tail} was plotted as a function of V_t and fitted with a Boltzmann function (smooth curves). For control, $V_{0.5} = -22.0 \pm 0.5$ mV; $k = 8.1 \pm 0.3$. For AZA1, $V_{0.5} = -20.7 \pm 0.5$ mV; $k = 9.6 \pm 0.3$ ($n = 6$).

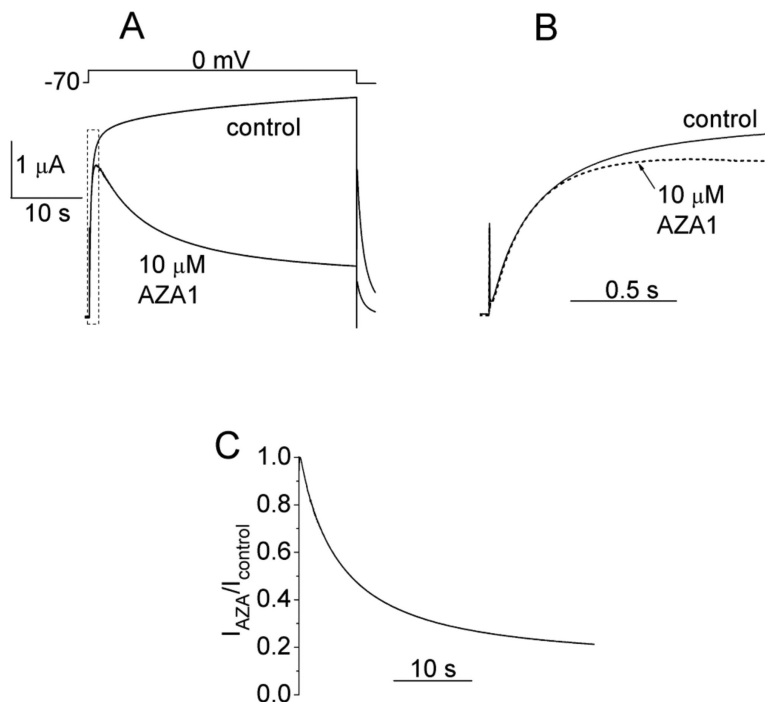


Figure 4.

AZA1 preferentially blocks hERG1 channels in the open state. (A) and (B) Superimposed traces of currents recorded before (control) and after a 4 min pulse-free period of incubation of oocyte with 10 μM AZA1. Currents were recorded in response to 37.8 s pulse to 0 from a holding potential of -70 mV. The complete current traces are shown in panel A and the region delineated by the dotted box (initial 1.34 s of pulse) is shown on an expanded time scale in panel B. (C) The ratio $I_{AZA1}/I_{control}$ plotted as a function of time during the pulse to 0 mV. The decay of $I_{AZA1}/I_{control}$ with time is a direct measure of the bi-exponential onset of current block with $\tau_{fast} = 2.96$ s (amplitude = 0.325) and $\tau_{slow} = 12.66$ s (amplitude = 0.433). The steady state relative current amplitude (0.192) represents the amount (19.2%) of unblocked current. R^2 for fit was 0.997.

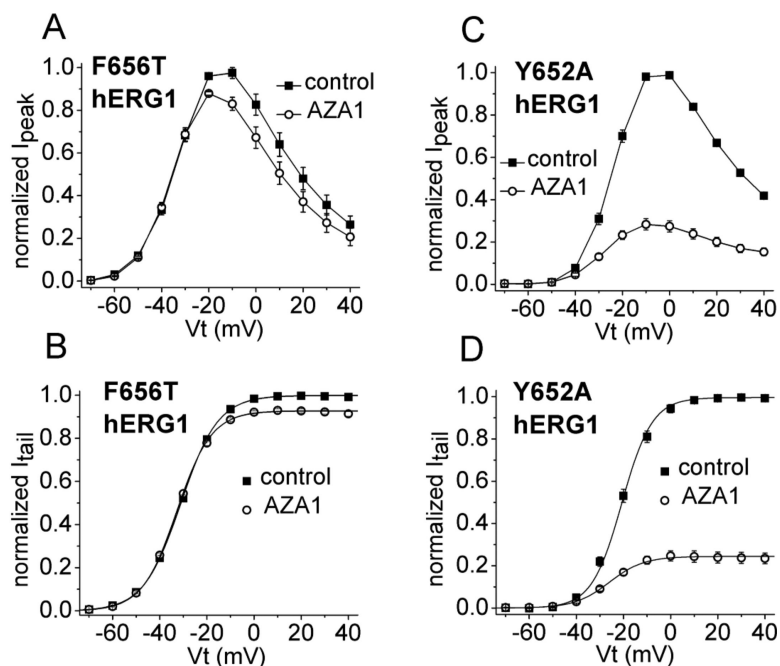


Figure 5.

Block of hERG1 by AZA1 is attenuated by mutation of F656 but not Y652. (A) Effect of 10 μ M AZA1 on the I - V_t relationship for F656T hERG1 channels. (B) Effect of 10 μ M AZA1 on the G - V_t relationship for F656T hERG1 channels. Normalized I_{tail} was plotted as a function of V_t and fitted with a Boltzmann function (smooth curves). For control, $V_{0.5} = -31.0 \pm 0.2$ mV; $k = 7.8 \pm 0.1$. For AZA1, $V_{0.5} = -32.6 \pm 0.3$ mV; $k = 7.3 \pm 0.1$ ($n = 5$). (C) Effect of 10 μ M AZA1 on the I - V_t relationship for Y652A hERG1 channels. (D) Effect of 10 μ M AZA1 on the G - V_t relationship for Y652A hERG1 channels. Normalized I_{tail} was plotted as a function of V_t and fitted with a Boltzmann function (smooth curves). For control, $V_{0.5} = -20.7 \pm 0.6$ mV; $k = 6.4 \pm 0.3$. For AZA1, $V_{0.5} = -26.0 \pm 0.8$ mV; $k = 7.3 \pm 0.4$ ($n = 5$).

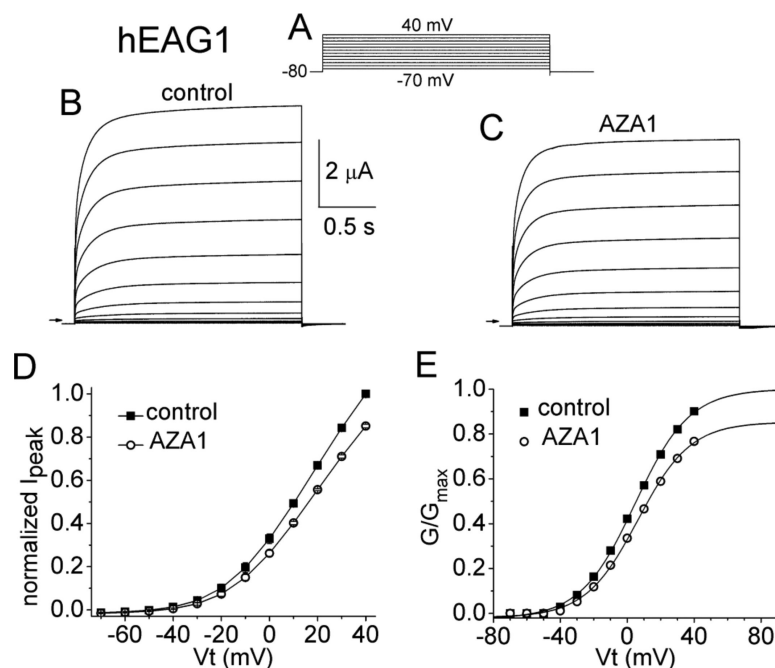


Figure 6.

AZA1 is a weak blocker of hEAG1 channels. (A) Voltage clamp protocol used to elicit currents illustrated in panels B and C. (B) Control hEAG1 currents. (C) Currents recorded in the presence of 10 μM AZA1. (D) Effect of AZA1 on the I - V_t relationship for hEAG1 channels. (E) Effect of AZA1 on the G - V_t relationship for hEAG1 channels. Normalized $I_{\text{peak}}/(V_t - E_{\text{rev}})$ was plotted as a function of V_t and fitted with a Boltzmann function (smooth curves). For control, $V_{0.5} = 4.6 \pm 0.7$ mV; $k = 16.3 \pm 0.6$. For 10 μM AZA1, $V_{0.5} = 6.4 \pm 0.9$ mV; $k = 15.7 \pm 0.7$ ($n = 4$).

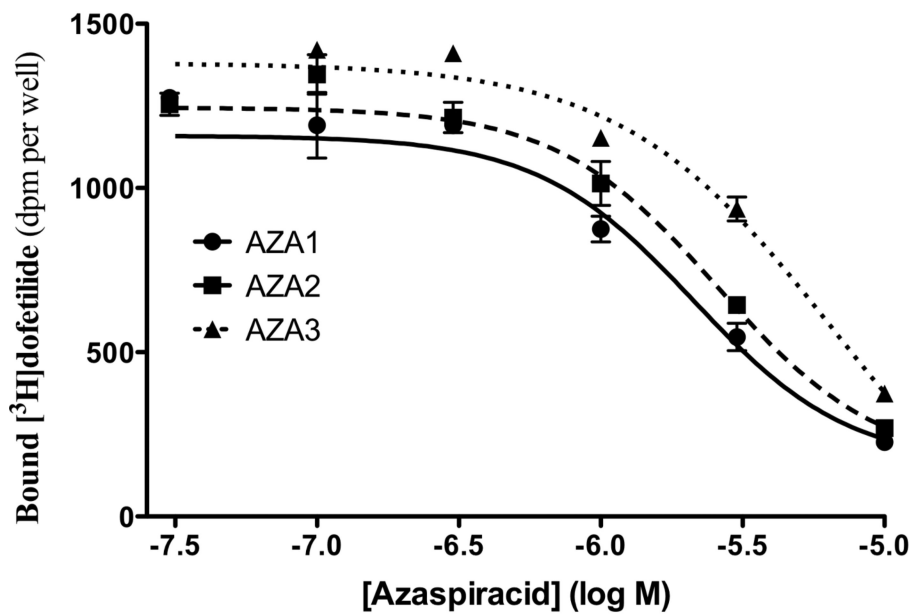


Figure 7. AZAs compete with dofetilide for hERG potassium channels. Various concentrations of AZA1, AZA2, and AZA3 were used as competitors in a [³H]dofetilide hERG channel binding assay. All data (mean ± SEM; n=3) were analyzed using non-linear sigmoidal dose-response. Dofetilide was used as a positive control. Calculated IC₅₀ values are shown in Table 1.

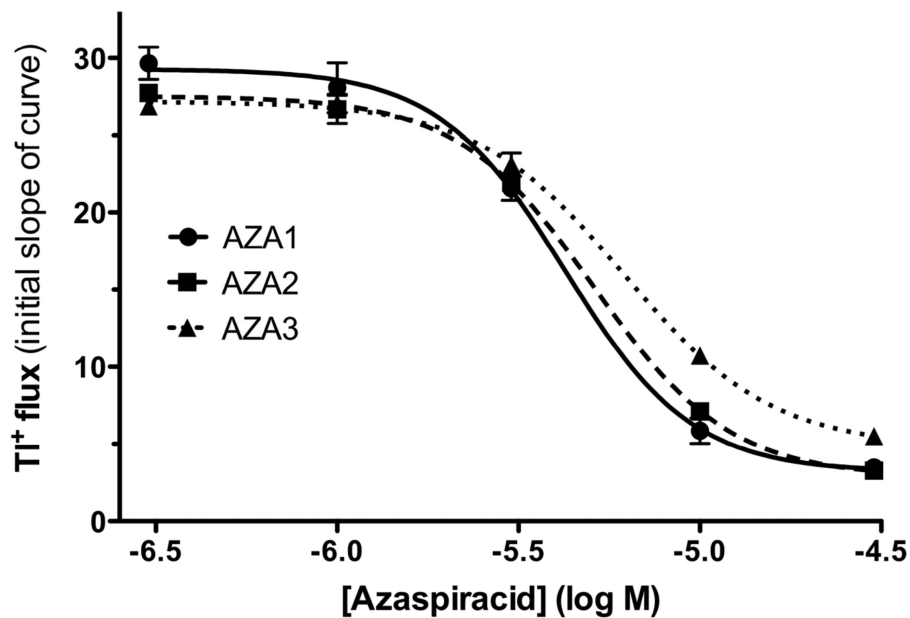


Figure 8. AZAs inhibit thallium flux through hERG potassium channels. Various concentrations of AZA1, AZA2, and AZA3 were tested using the thallium (Tl^+) flux assay. All data (mean \pm SEM; n=3) were analyzed using non-linear sigmoidal dose-response. Terfenadine was used as a positive control. Calculated IC_{50} values are shown in Table 1.

hERG inhibition IC₅₀ values (in μ M) and 95% confidence intervals (CI) for AZA1, AZA2, and AZA3 as determined using patch clamp, channel binding, and thallium flux assays. The relative potency of each compound is compared to AZA1.

Table 1

Assay	AZA1			AZA2			AZA3			Terfenadine ^a /Dofetilide ^b		
	Mean	95% CI	Rel. Pot.	Mean	95% CI	Rel. Pot.	Mean	95% CI	Rel. Pot.	Mean	95% CI	Rel. Pot.
Patch Clamp	0.84	0.76 - 0.93	1.0	0.64	0.58 - 0.70	1.3	0.84	0.72 - 0.97	1.0	0.019	0.016 - 0.022 ^a	44.2
Channel Binding	2.1	1.2 - 3.8	1.0	2.6	1.6 - 4.2	0.8	6.6	0.97 - 44.5	0.3	0.0088	0.0063 - 0.012 ^b	238.6
Thallium Flux	4.2	3.4 - 5.3	1.0	5.1	4.5 - 5.8	0.8	6.2	5.4 - 7.0	0.7	8.4	6.7 - 10 ^a	0.5